



Modeling the impact of rainfall variations and management interventions on the groundwater regime of a hard-rock terrain in central India

Ranjan K. Ray¹ · Tajdarul H. Syed² · Dipankar Saha¹ · Bhabesh C. Sarkar²

Received: 21 July 2019 / Accepted: 10 February 2020 / Published online: 13 April 2020
© Springer-Verlag GmbH Germany, part of Springer Nature 2020

Abstract

Realistic assessment and prediction of groundwater resources, at appropriate scales, are crucial for proper management and systematic development of groundwater in India. An equivalent porous medium (EPM)-based groundwater flow model is implemented for a typical hard-rock aquifer in central India, to provide quantification, analysis and prediction of groundwater balance components. This research also provides refined estimates of aquifer parameters, recharge factors and newer insights into groundwater dynamics. It is observed that evaporative losses and effluent seepage of groundwater to rivers jointly account for ~20% of the annual recharge, which is significantly higher than most prior regional assessments. Evaluation of groundwater resource use under a business-as-usual scenario shows annual groundwater draft to exceed recharge by 13% in the year 2020–2021, and under a worst-case scenario (with prevailing drought conditions) this deficit is predicted to increase to 30%. However, with suitable recharge augmentation and demand control measures, in the best-case scenario, groundwater draft can be contained to ~90% of annual recharge, thereby ensuring long-term sustainability of groundwater resources. Importantly, this study reveals that demand control measures can be more effective than recharge augmentation measures.

Keywords India · Hard-rock terrain · Carbonate rocks · Groundwater management · Numerical modeling

Introduction

Groundwater has emerged as an increasingly important common-pool resource that is under continuous stress in India (Famiglietti 2014). According to a recent estimate (CGWB 2019), groundwater extraction in India ($\sim 249 \times 10^9 \text{ m}^3$), the majority of which is used for irrigation only, is more than one third of the total groundwater extraction of the world (FAO 2016). Further, nearly 17% of the 6,881 groundwater assessment units in the country have been classified as ‘overexploited’, a majority of which are located in the peninsular region of India. Peninsular India, with

an area of ~ 2 million km^2 , is mainly comprised of hard-rock aquifers that have limited groundwater potential and pose additional challenges in terms of heterogeneity in hydrogeologic properties (Singhal and Gupta 1999). Though groundwater management is an immediate requirement in the hard-rock areas of peninsular India, it is severely constrained by the lack of proper understanding and absence of tools for informed decision making.

Groundwater flow modeling has been widely used as an effective tool for studying groundwater dynamics (Anderson and Woessner 1992; Zhou and Li 2011); however, hard-rock aquifers, including carbonate aquifers, impose certain limitations owing to aquifer heterogeneity, dominance of secondary (fractures) or tertiary (conduits) porosity and existence of a hierarchical permeability structure or flow paths (Scanlon et al. 2003). Notwithstanding these limitations, useful numerical flow models can be developed in hard-rock aquifers, as long as their limitations are acknowledged and duly represented in the model (Quinlan et al. 1996)—for example, discrete fracture network or dual porosity modeling approaches can be used in karst/fracture aquifers (NRC 1996). These approaches, however, require exhaustive details on aquifer properties,

✉ Tajdarul H. Syed
tsyed@iitism.ac.in

¹ Central Ground Water Board (CGWB), BhujalBhawan, NH-IV, Faridabad, India

² Department of Applied Geology, Indian Institute of Technology (ISM), Dhanbad, India

including that of fractures, which are extremely difficult to obtain on appropriate modeling scales. Alternatively, an equivalent porous medium (EPM) approach has been efficiently implemented for regional aquifer systems with dense, interconnected fractures and voids (Abbo et al. 2003; Anderson and Woessner 1992; Huntoon 1994; Romanazzi et al. 2015; Scanlon et al. 2003; Surinaidu et al. 2013; Yao et al. 2015). The EPM approach, which is also adopted in this study, is considered to be most reliable for regional-scale simulations (Langevin 2003; Schwarz and Smith 1988). This approach is particularly appropriate for resource management purposes, in which greater emphasis is given on the overall assessment of groundwater resources rather than its variation in space (Panagopoulos 2012; Schwarz and Smith 1988; Smith and Schwarz 1984). Scanlon et al. (2003) specifically showed that regional groundwater flow simulated using an EPM approach can be critical for groundwater resource management.

In India, groundwater flow modeling studies have been largely restricted to unconsolidated (alluvium) or semiconsolidated (Gondwana) sedimentary terrains. These modeling studies have addressed a variety of issues including groundwater flow dynamics (e.g. Ahmad and Umar 2009; Alam and Umar 2013; Kushwaha et al. 2009; Sahoo and Jha 2017), arsenic contamination and migration (Mukherjee et al. 2007; Sikdar and Chakraborty 2017) and groundwater seepage to coal mines (Surinaidu et al. 2014). Groundwater flow modeling studies in hard-rock areas of India are limited and those that exist are from granitic terrains only (e.g. Ahmed et al. 2003; Thangarajan 1999). Also note that, thus far, all the modeling studies have either been restricted to the alluvial terrains of northern and eastern parts of India (e.g. Ahmad and Umar 2009; Alam and Umar 2013; Kushwaha et al. 2009; Mukherjee et al. 2007; Sahoo and Jha 2017; Sikdar and Chakraborty 2017) or the hard-rock areas of southern India (Ahmed et al. 2003; Thangarajan 1999). In view of the information required for planning and management of groundwater resources and the existing knowledge gaps, this study develops a groundwater flow model for the Seonath Kharun Interfluvium (SKI) area in central India. In this region the principal aquifer is comprised of Precambrian calcareous sediments. To the best of the authors' knowledge, this is the first groundwater flow model for any carbonate aquifer in India. With an overall aim to support decision making for groundwater management, the specific objectives of this study are: (1) integration of available information on hydrogeological characteristics and stresses, (2) development of an operational groundwater flow model, for refinement of available estimates of hydrogeological parameters and stresses, and (3) analysis and prediction of future groundwater scenarios using the newly developed groundwater flow model.

Study area

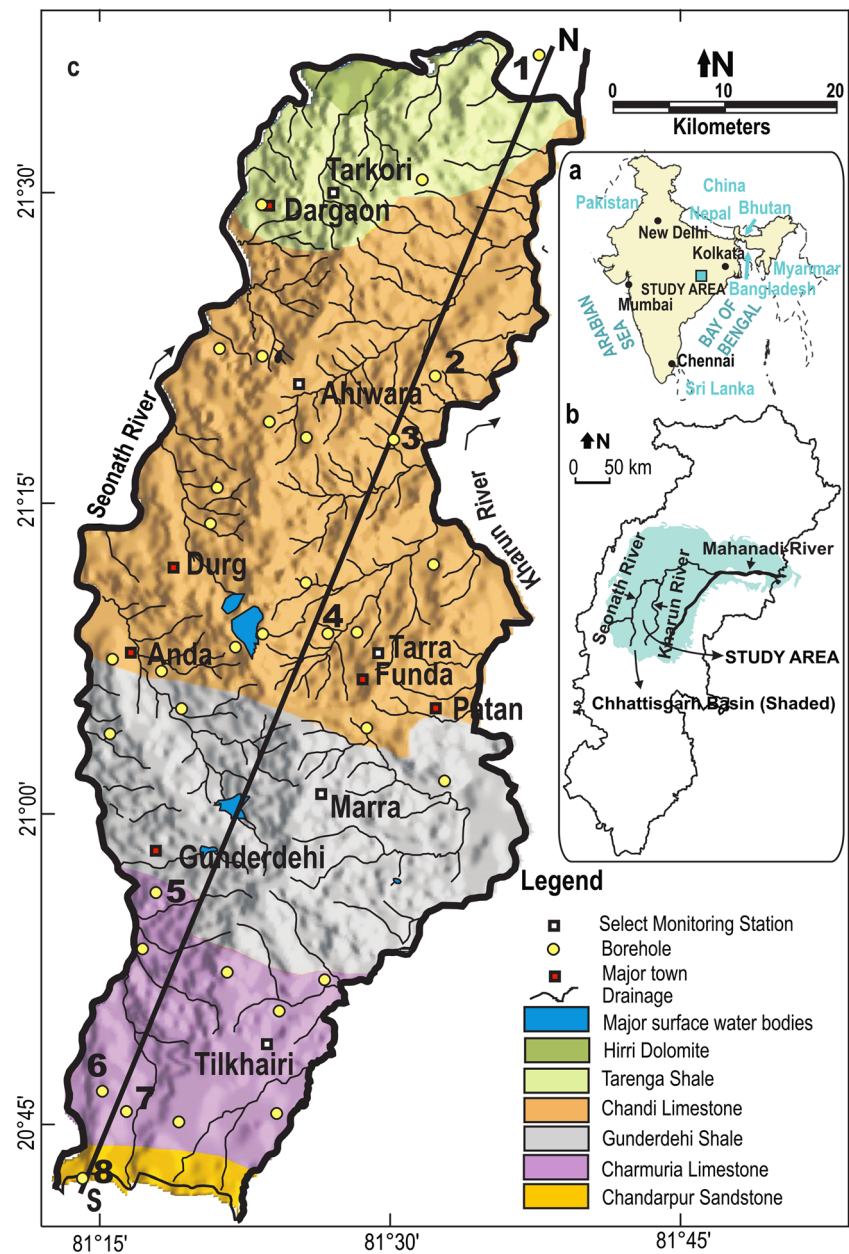
The study area (Fig. 1) located in central India, between 81° 13' and 81° 40' E longitudes and 20° 40' and 21° 38' N latitudes, covers 2,867 km² of the undivided district of Durg (now split into three districts: Balod, Durg and Bemetara) in the state of Chhattisgarh. Two ephemeral streams, Kharun and Seonath, which are tributaries to the Mahanadi River, define the eastern and the western boundaries of the study area respectively. Elevations in the area vary from 258 to 337 m above mean sea level (amsl), with a maximum slope of 4%. The total population is nearly 1.8 million with an overall density of ~630 persons per km². The populace in rural areas and in the small towns is almost entirely dependent on groundwater for domestic purposes, whereas in the urban areas (Durg Municipal Corporation), groundwater caters for up to 50% of domestic water supply.

The area experiences a subtropical climate with short winters (2 months) and prolonged summers (4 months). December and January are the coldest months in a year and the daily lowest temperatures during these months remain mostly around 15 °C. Highest temperatures in the range of 45 °C are recorded in the month of June, which is the hottest month. Average annual rainfall (for the period 2000–2014) in the area is 1,050 mm and is mostly attributed to the SW monsoon. More than 90% of the annual rainfall is restricted to 4 months (June–September) in a year, which is denoted as the monsoon season.

The entire year can be broadly divided into two cropping seasons: kharif (mid June to early November) and rabi (end of November to mid April). During peak summer (Mid April to mid June) usually no irrigated crops are grown. The principal crop grown in the kharif period is rice and it is largely rain-fed; however, canal water and groundwater have to be utilized for irrigation during intermittent dry spells even in the monsoon period. Rice, wheat, legumes and oilseeds are grown during the rabi period, of which legumes and oilseeds do not require additional irrigation, while rice and wheat are almost entirely irrigated from groundwater. The sown area during the kharif period and double cropped area (area sown both in kharif as well as rabi period) accounts for 57 and 19% of the geographical area respectively.

Out of the seven groundwater assessment units, parts of which constitute the study area, one unit had been reported to be overexploited and four other units were categorized as semicritical (CGWB 2017a). Periodic assessments of groundwater resource availability and utilisation, undertaken by Central Ground Water Board (CGWB 2006b, 2011, 2014, 2017a), have revealed consistent increase in groundwater withdrawal in the area. Ray et al. (2017a) predicted a 6% annual increase in groundwater draft for irrigation during the period 2013–2020. At this rate, major parts of the SKI region may become water stressed by 2020 and therefore require immediate management interventions. Some of the prior studies in the region include district-wise estimation of the water

Fig. 1 **a** Location, **b** drainage and **c** topography and geology of Kharun-Seonath interfluvial area, Chhattisgarh State, India. Geological section along the line N–S is shown in Fig. 2. Numbers along the section line indicate the locations of the boreholes (1 Raka, 2 Gudheli, 3 Kapasada, 4 Purena, 5 Kachandur, 6 Latabod, 7 Padkibhat and 8 Jhalmala)



sustainability index (WSI; Kansal and Chandniha 2015), delineation of a groundwater potential map (Kumar and Gautam 2014) and estimation of the specific yields of two lithological units on the basis of dry-season water-balance computation (Ray et al. 2014). It is only recently that Ray et al. (2017b) presented a detailed analysis of major ion chemistry and stable isotope ratios of groundwater in order to establish its hydrogeochemical characteristics and dominant recharge mechanisms, and to provide an estimate of rainfall infiltration on the basis of chloride mass balance. Thereafter, Ray et al. (2017a) presented a comprehensive assessment and prediction of fine-scale groundwater draft for irrigation in the current study area. Still, there are apparent deficiencies in the estimates of important stresses, like evapotranspiration losses

from groundwater through the plants and effluent seepage to rivers, at scales most essential for effective planning and management of groundwater resources. Furthermore, the prior studies, as summarized in the preceding part of this section, dealt with specific groundwater issues but none provided a comprehensive assessment of water resource availability and utilization, which is critical to determine the limits of sustainable use and ensure adequate supply of freshwater in future.

Hydrogeologic framework

The Chhattisgarh basin, a Precambrian sedimentary basin, is spread over $\sim 33,000$ km² area in the central part of

Chhattisgarh State (Fig. 1). The unmetamorphosed Precambrian sediments which fill the Chhattisgarh Basin are designated as Chhattisgarh Super Group of rocks; Archaean to Lower Proterozoic granitoids form the basement of the Chhattisgarh basin. These granitoids are overlain by sediments that comprise a lower arenitic sequence vertically grading to an argillite-carbonate suite. The lower arenitic sequence has been designated as the Chandarpur Group and the upper cyclic argillite carbonate suite has been named as the Raipur Group (Das et al. 1992). The Raipur Group has been subdivided into six formations representing three cycles of carbonate-argillite sedimentation—i.e. Charmuria and Gunderdehi, Chandi and Tarenga, and Hirri and Maniari, arranged in an ascending order of superposition (Das et al. 1992; Mukherjee et al. 2014). Significant facies variations are observed even within the individual geological formations. On a basin scale, in terms of hydrogeological properties, the rock formations in the study area can be grouped into six hydrostratigraphic units: (1) Chandarpur Sandstone, (2) Charmuria Limestone, (3) Gunderdehi Shale, (4) Chandi Limestone, (5) Tarenga Shale, and (6) Hirri Dolomite. The distribution of hydrostratigraphic units (Mukherjee et al. 2014) is shown in Fig. 1.

The Central Ground Water Board (CGWB) has constructed more than 350 exploratory boreholes in the Chhattisgarh Basin (CGWB 2006a), of which 43 are located in the study area. These 43 boreholes in the study area have been drilled in 31 different locations (Fig. 1), including more than one borehole at some locations. Figure 1 also shows the locations of one borehole each in Chandarpur Sandstone and Tarenga Shale that are outside the study area, but have been considered for the construction of a lithological cross section (Fig. 2). These boreholes vary in depth from 60 to 300 m. Information regarding the disposition of the hydrostratigraphic units is derived from the available lithologies. Though the depths of the units vary up to 670 m (Mukherjee et al. 2014), potential water bearing zones are restricted to the top 150 m only. In the Gunderdehi (shale) unit, water-bearing zones are restricted mostly to the upper weathered part. The Chandarpur Sandstone unit is highly silicified and as such has

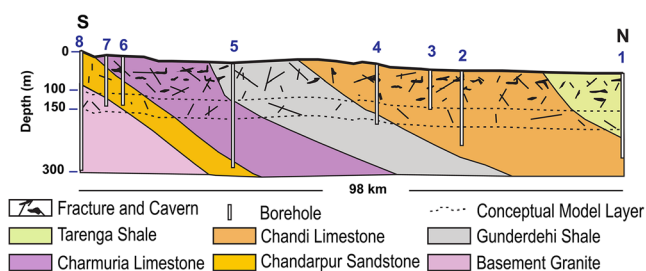


Fig. 2 Hydrogeological cross section and a conceptual model of the study area. The numbers indicate location of boreholes drilled by Central Ground Water Board (1 Raka, 2 Gudheli, 3 Kapasada, 4 Purena, 5 Kachandur, 6 Latabod, 7 Padkibhat and 8 Jhalmala). The section line is shown in Fig. 1. The geological units have a very low dip. The apparent dip seen in the section is because of high vertical exaggeration (1:60)

very limited porosity. Solution cavities are the predominant controls of groundwater occurrence and movement in Charmuria Limestone, Chandi Limestone, Hirri Dolomite and Tarenga Shale units. The well productivities (specific capacity per unit saturated thickness) in such terrains usually decrease with depth due to decrease in fracturing and solution activity (Walton 1970). A similar trend is also observed in the Chhattisgarh basin (Khare 1981; Singhal and Gupta 1999). Available drilling data of CGWB as summarised in Table 1 shows that yield characteristics of the hydrostratigraphic units are comparable. ‘Drill-time discharge’ as summarised in the table represents the yield characteristics or relative potential of the aquifers (Kaehler and Hsieh 1994). Except for the wells with very high yields (>10 L/s), well-defined fracture/cavernous zones are not apparent. The limestone and calcareous shale formations in the study area represent impure carbonates, which do not develop distinct karst landforms (Ford and Williams 2007). This is evident from the available lithologies in which caverns are observed to be usually small and closely spaced. Also, typical karst features like sinkholes or springs are practically nonexistent in the area. The predominant (~60%) soil type in the study area is clay loam, the others being gravelly clay loam, gravelly sandy clay loam, gravelly sandy loam and sandy clay loam (Kumar and Gautam 2014). Chemical and isotopic studies (Ray et al. 2017b) show that monsoon rainfall is the primary source of recharge and recharge is rapid, that is without significant evaporative enrichment. Isotopic analysis (Ray et al. 2017b) of surface water and groundwater samples show that active intermixing of surface and groundwater resources is not a predominant process. Isotopic signatures of groundwater samples collected from wells of different depth are comparable to each other indicating that the aquifers are vertically connected. The hydrostratigraphic framework as adopted in the numerical model is shown in Fig. 2.

Major sources of data

The hydrogeological framework used in this study is derived primarily from the lithologies obtained from boreholes drilled by CGWB. Hydraulic conductivity values were derived from pumping test data available with CGWB, which are archived in their local office (North Central Chhattisgarh Region, Raipur) and summarized in CGWB (2006a, 2012). Initial storage parameters are assigned to different hydrostratigraphic units based on the available field estimates of specific yield (Ray et al. 2014). Observations of river stage, river discharge and water released through the canals used for irrigation are obtained from the Water Resources Department of the Government of Chhattisgarh State. Also used in the flow model are field-based estimates and projections of village-wise groundwater draft for irrigation in the study area for the period 2013–2014 to 2020–2021 (Ray et al. 2017a). Monthly rainfall data are obtained from India Meteorological Department

Table 1 Characteristics of major hydrostratigraphic units in the study area (Ray et al. 2017b). bgl below ground level

Hydrostratigraphic units (percentage of study area covered)	Major lithologies	Maximum thickness ^b	Number of wells drilled in the study area	Water bearing zones and yield characteristics	Yield characteristic (max. drill time discharge)		Depth to water level range (m bgl)	
					May	Sept	May	Sept
^a Hirri Dolomite (~1%)	Dolomite	150 m	–	Mostly restricted to 70 m bgl, rarely up to 130 m bgl	5 L/s	3.45–10.19	1.36–6.53	
Tarenga Shale (~11%)	Calcareous Shale	>300 m	3	Deepest zone encountered at 183 m bgl; majority within 70 m bgl	17 L/s			
Chandi Limestone (~44%)	Limestone with shale intercalations	670 m	26	Deepest 152 m bgl, mostly restricted to 35 m bgl	12 L/s	1.28–15.1	0.75–6.53	
Gunderdehi Shale (~27%)	Shale	>300 m	3	No zones in one well. In the remaining two, the zones were within 20 m bgl	3.5 L/s	1.5–10.75	0.8–3.02	
Charmuria Limestone (~15%)	Dominantly carbonate sequence	260 m	11	Deepest 84 m bgl, mostly within 30 m bgl	15 L/s	1.65–11.45	0.77–7.23	
^a Chandarpur Sandstone (~2%)	Orthoquartzite arenites/sandstones	130 m	–	Mostly the upper weathered part; occasionally contact with granitoids. Depth of this contact varies up to 130 m bgl	1 L/s	5.41–9.05	2.83–4.05	

^a Lithologies of wells representing Hirri Dolomite and Chandarpur Sandstone in the study area are not available. The information given here is based on available lithologies in adjacent areas as summarised in CGWB (2006a)

^b Mukherjee et al. 2014

(IMD). Preliminary input into the model also includes water level data from a network of 79 groundwater monitoring wells and two river stage monitoring locations (Fig. 3). Groundwater levels and river stages have been regularly monitored since 2010. Since there are no previous estimates of evapotranspiration (ET) losses from groundwater available for the study area, in this study, it is estimated from available reference ET values (Kumar 2014) by integrating landuse data, soil characteristics and depth to water table using the methodology suggested by Shah et al. (2007).

Groundwater model setup

Model design, boundary conditions and aquifer parameters

Groundwater flow modeling requires simplifications due to the inherent complexity of stratigraphic systems. A simplified

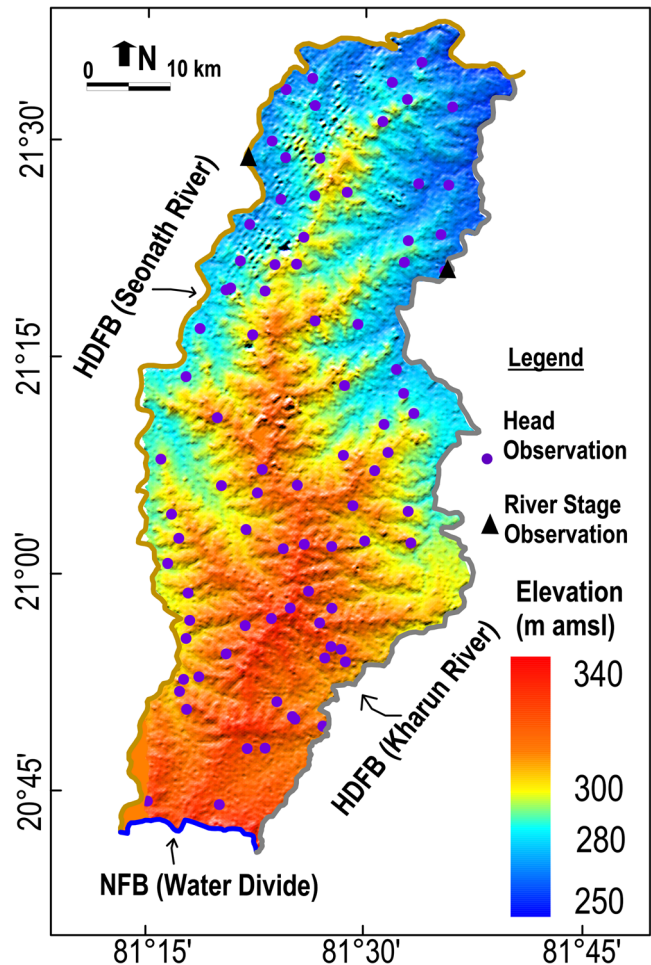


Fig. 3 Model domain with boundaries. Elevations as shown here are extracted from SRTM (90 m) DEM. Locations of 79 head observation points and 2 river stage observation points are also shown. HDFB head-dependent flow boundary; NFB no-flow boundary

hydrostratigraphic framework (Fig. 2), as described in the previous section, forms the fundamental basis for groundwater flow model development. In this study, groundwater flow is simulated using a block-centered finite difference grid using MODFLOW 2000 (Harbaugh et al. 2000). In fractured and karstic aquifers, the size of grid in the model should be large enough to grossly approximate equivalent porous media (Neuman 1987; Pankow et al. 1986). Hence, the model domain is discretized into 2,867 square grids of 1-km² size (1 km × 1 km), based on the availability of data on essential hydrogeological parameters, and the flexibility and stability of selected codes in accordance with the EPM hypothesis. Maximum length (along N–S) and breadth (along E–W) of the model domain is 100 and 50 km respectively. Surface elevations derived from Shuttle Radar Topography Mission (SRTM) Elevation Dataset (with 90-m resolution) is used to define the topography. As observed from available borehole lithologies and as also reported by other authors (Khare 1981; Singhal and Gupta 1999), density of fractures/solutions cavities and consequent well productivity goes on decreasing with depth in the study area. Water bearing zones are practically absent beyond 150 m below ground level irrespective of the hydrostratigraphic unit. Accordingly, the thickness of the model domain has been taken as 150 m. Further, based on the disposition of the rock types in the available lithologies, the vertical model domain is discretized into two layers as shown in the lithological cross-section (Fig. 2). The upper layer (with a relatively higher conductivity) is considered as a layer with a constant thickness of 100 m (from ground level) followed by a deeper layer (with lower conductivity) of 50 m thickness. Two rivers, Seonath and Kharun act as boundaries of the study area on the west, east and northern parts. These rivers are modeled as head dependent flow boundaries. A representative hydrograph of river discharge for Kharun River measured at Amdi site for the year 2010 shows that the river is active only during July to September (Fig. 4). Monthly observations of river stage, monitored at two locations (one each on Kharun River and Seonath River), are assigned as observed heads for the rivers. The southern boundary of the model domain is a well-defined water divide. Furthermore, this divide is located

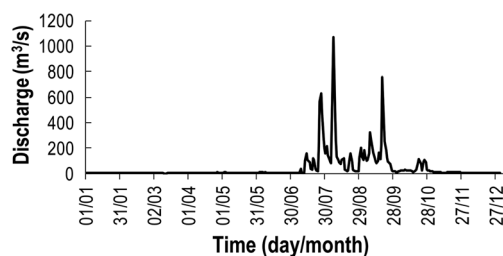


Fig. 4 Hydrograph showing daily variations in river discharge recorded at Amdi gauging site on Kharun River for a representative year (2010). The data were obtained from State Water Resources Department, Govt. of Chhattisgarh

within a highly silicified Precambrian Sandstone (orthoquartzite), which is a poor aquifer with restricted groundwater flow. This water divide is adopted as a ‘no-flow’ boundary (Fig. 3). The model domain is also rotated by 15° towards the west in order to align the principal axes of the model domain with the major flow directions.

The Central Ground Water Board (CGWB), as a part of its exploratory drilling program, has constructed 43 boreholes in the study area over the last four decades, from which transmissivity values are available from 12 constant-discharge pumping tests carried out by CGWB in boreholes at 12 locations. Pumping durations varied from 100 to 400 min, and pumping rates ranged from less than 10 m³/day to more than 600 m³/day. Given the large range in transmissivity values, the available data, which are few and far between, may not represent the spatial variation of transmissivity (or hydraulic conductivity) values adequately. However, since there is a good correlation between well yield and hydraulic conductivity, discharge from wells measured during drilling can be used as a surrogate of hydraulic conductivity (Chatterjee and Ray 2016; DWAf 2006). Kaehler and Hsieh (1994) had used well discharge as a tool for comparison of yield characteristics of different hydrostratigraphic units. Hence, in this study, distribution of well discharges is used as an additional control and the study area is divided into five different zones, each representing different hydraulic conductivities. In the absence of specific information, hydraulic conductivity of the second layer has been considered to be half of that of the corresponding upper layer. The aquifer is assumed to be isotropic in the horizontal plane ($K_x = K_y$) and the vertical hydraulic conductivity is assumed to be 10% of horizontal conductivity. Ray et al. (2014), based on a dry season water balance approach applied to a set of watersheds adjacent (along the southeastern boundary) to the study area, had estimated the specific yield (S_y) of Chandarpur Sandstone to be 0.0038 and that of Charmuria Limestone to be 0.04. No other field estimate of specific yield is available for the study area. These hydraulic conductivity and specific yield values are used as initial inputs and later refined using the PEST module of Visual MODFLOW. The aquifer properties, boundaries and recharge-discharge components are manually assigned to individual grid cells or a group of grid cells (zones) as the case may be. Surface elevation values, elevations of layer boundaries and initial heads are imported from ASCII files and necessary interpolations are done in Visual MODFLOW using the natural neighbors interpolator.

Sources and sinks

The primary sources of recharge in the study area are rainfall (R_{rf}), return flow from groundwater-based irrigation (R_{irr}) and canal water (R_{canal}). Ray et al. (2017b), based on chloride mass balance, estimated the annual recharge rates (R_{rf} as percentage

of annual rainfall) to be 4.5% for Chandi and Charmuria units, 1.8% for Gunderdehi unit and 2.2% for Tarenga and Hirri units. Since no analytical data are available for Chandarpur Sandstone, the recharge factor of Chandarpur Sandstone is assumed to be similar to the Gunderdehi Unit, based on the similarity of their hydrogeological potential. Monthly rainfall records for the district are obtained from India Meteorological Department (IMD). Based on monthly rainfall and recharge factors, initial recharge rates are applied to the model. Since there are no specific studies detailing the quantification of return flow rates from groundwater-based irrigation and recharge from canal water discharged to the study area, the generalized norms were followed for recharge estimation in India (MoWR 2009). Return flow from groundwater irrigation is negligible during July and August since the region receives the highest rainfall during these two months. Scope for additional recharge (from groundwater irrigation return flow) besides rainfall recharge is negligible during this period. On the other hand, during the remaining months, return flow from irrigation is significant. For this period (September to June), 50% of groundwater extraction for irrigation and 30% of canal water is considered as recharge to groundwater.

Obtaining reliable estimates of groundwater extraction has been a major limitation for comprehensive groundwater resource assessment in India (Chatterjee and Ray 2016). In the study area, groundwater utilization is mostly for irrigation purposes followed by domestic use. Groundwater extraction for industrial use is negligible (Ray et al. 2017a). Earlier, Ray et al. (2017a) reported village-wise estimates of groundwater draft for irrigation in the study area and its projection for the period 2013–2021. These draft estimates were based on the number of abstraction structures, measurement of instantaneous discharge from wells in the field and feedback from the local farmers. According to these estimates, annual groundwater extraction for irrigation in the study area during the water year 2013–2014 was $212 \times 10^6 \text{ m}^3$, which was projected to increase to $307 \times 10^6 \text{ m}^3$ in the year 2020–2021, at an average rate of 6% per year. Groundwater draft for domestic purposes (D_{dom}) is estimated using the population census of the Government of India and per capita per day (liters per capita per day, lpcd) consumption of water. The per capita water consumption varies from ~60 lpcd in rural areas to ~120 lpcd in urban areas. Domestic draft is projected to the water year 2020–2021 based on annual population growth rate. Subsequently, domestic draft is added to irrigation draft and the total groundwater draft is incorporated in the model. For the entire study area, groundwater draft for domestic use is estimated to be $31 \times 10^6 \text{ m}^3$ for the year of study (2013–2014) and projected to be $34 \times 10^6 \text{ m}^3$ for 2020–2021, an increase of nearly 10% over a period of 8 years. Recharge from the rivers (R_{riv}) and effluent seepage to rivers (D_{riv}) are assessed using the groundwater flow model utilizing limited observations of river stages and river bed conductance. River bed conductance

(R_C) has been approximated from hydraulic conductivity of the riverbed (K), channel width (W), length of the channel segment (L) and thickness of the riverbed sediment (T) using the conductance formula (Eq. 1; SWS 2010)

$$R_C = \frac{K \times W \times L}{T} \quad (1)$$

The values thus estimated range between 2,000 to 3,000 m^2/day . Loss of groundwater through evapotranspiration (ET_{gw}) is one of the important components of water balance computation (Narasimhan 2008; Shah et al. 2007; White 1932). More particularly, in the context of the study area where summer temperatures go up to 45 °C, the water table, in general, remains at a shallow depth. Due to the nonavailability of ET_{gw} estimates for the study area, ET_{gw} is estimated from available reference evapotranspiration values (Kumar 2014) using the partitioning factors, which in turn are estimated using the methodology proposed by Shah et al. (2007). Following this methodology (Shah et al. 2007), spatially distributed ET_{gw} partitioning factors are approximated using soil type, vegetation type, groundwater level and landuse pattern. Estimated annual ET_{gw} varies from being negligible, in areas with deep water level, to as high as ~1 m/year in agriculture fields with shallow water table. The ET_{gw} thus estimated is incorporated as a key hydrologic flux in the groundwater flow model developed here.

Model execution and calibration

In view of prevailing monsoon conditions, the water year in India is considered to span from July through June (Rhode et al. 2015). In the present study, the beginning and end of a water year is considered to be the 1st of July and the 30th of June, respectively—for example, the water year 2013–2014 refers to the period from 1 July 2013 to 30 June 2014. The model is executed for a period of 8 years (2013–2014 to 2020–2021) starting from 1 July 2013. Before implementing the model in transient mode, it was run with a steady-state dataset. While it is difficult to assume a true steady-state condition, as suggested by Anderson and Woessner (1992), it might be more appropriate to assume that water levels measured during a certain period represent quasi steady-state conditions under stresses that prevail during that period. Analysis of monthly water levels in the study area shows that changes in depth to water level during the months of July to August, in almost all the wells, are negligible. Thus, prevailing conditions during this period (July–August) can be considered to be ‘steady state’ for the present flow modeling purpose. Accordingly, the steady-state dataset for this study comprised of recharge rate, groundwater draft, groundwater levels and other parameters for the month of July, averaged over the period 2013–2017. Observed water levels from a network of

79 wells for the said period are considered as calibration targets. Since most of the observed data are available on a monthly basis, stress period during model execution is taken as 30 days (~1 month). Model calibration is performed in two stages, manual calibration is followed by automated calibration. Manual calibration is performed for both steady-state and transient-state simulations. The model is first calibrated using the steady-state dataset. During steady-state calibration, only the hydraulic conductivity values are systematically changed to improve the match between observed and calculated heads. Calibration is performed by manually changing the storage parameters and recharge rates. After the manual calibrations, automated model calibration is implemented, using the parameter optimization module of Visual MODFLOW (WinPEST) in order to improve the model results. During automated calibration, all the hydraulic conductivity and storage parameters are considered together for optimization. All the 79 observation wells (with weightage of 1) are used for defining the objective function. The ability of the model to reproduce the observed groundwater levels is quantified using root mean squared error (RMSE; Eq. 2).

$$\text{RMSE} = \sqrt{\frac{1}{n} \sum_{i=1}^n (X_i^{\text{calc}} - X_i^{\text{obs}})^2} \quad (2)$$

where n is the number of observations considered for calibration. X_i^{calc} , X_i^{obs} are the calculated and observed water-table elevations in an observation well, respectively.

Calibration during the transient state run is performed against observed water levels for the period June 2013 to November 2016. Using the predicted groundwater draft (Ray et al. 2017b), the model is run for the next 4 years (from 2016–2017 to 2020–2021) for prediction under different scenarios. Predicted water levels are further validated based on water levels collected from five locations for 2 years, 2017 and 2018. Monitoring stations at these five locations (Fig. 1) are part of the country-wide water level monitoring network maintained by CGWB from which water levels are collected four times a year.

Different test scenarios

The groundwater model thus developed is first implemented assuming normal rainfall conditions. Here, normal rainfall is defined according to the norms set by India Meteorological Department (IMD), which is rainfall ranging between $\pm 10\%$ of the long-term average (IMD 2020). Thereupon, model response is simulated by running the model under different stress conditions described in the following (Table 2):

1. *Drought condition.* As described in the previous section, the model is executed for eight water years with 2020–2021 (July 2020–June 2021) as the final water

year. To test the response of the system to drought conditions, year 2020–2021 is considered a drought year. As per the criteria adopted by Indian National Commission on Agriculture (Gupta et al. 2011), 25% deficit in rainfall is considered as meteorological drought. Accordingly, rainfall (and consequent recharge) in every month of the year 2020–2021 is taken as 75% of that in a normal rainfall year. In addition to the preceding, since the river flows are expected to decline during a drought year, river stages are assumed to be 0.5 m less than that during a normal rainfall year.

2. *Surplus rainfall.* Similarly, the final water year 2020–2021 (July 2020–June 2021) in the model is assumed to be a surplus rainfall year with 25% more rainfall compared to normal rainfall. Accordingly recharge in every month is considered to be 25% more than that during years with normal rainfall. Since surface runoff is also expected to increase during a surplus rainfall year, river stages are considered to be 0.5 m higher than that during a normal rainfall year. Analysis of annual rainfall data from Raipur rain gauge station in Kharun subbasin, as provided in Chandraprakash (2017), indicates five instances of deficit annual rainfall (annual rainfall $\leq 75\%$ of normal rainfall) and six instances of surplus annual rainfall (annual rainfall $\geq 125\%$ of normal rainfall) during the period 1975–2015 (41 years). Hence the probability of the year 2020–2021 being a surplus or deficit rainfall year is almost equal.
3. *Supply-side intervention.* While many managed aquifer recharge (MAR) interventions are possible (CGWB 2013), desilting of the existing waterbodies has been considered as a feasible and effective mode of increasing recharge in the area. Hydrochemical and stable isotope studies (Ray et al. 2017b) have shown that there is no active intermixing of surface and groundwater even in the vicinity of the ponds, which is possibly because of siltation in the ponds and tanks. Therefore, desilting may enhance the seepage rate from these waterbodies and subsequently augment the available groundwater resources. Since area-specific field observations are not available, recharge from desilted ponds is estimated by the following empirical relation (MoWR 2009).

$$R_{\text{pond}} = \text{Area} \times n \times \text{RF} \quad (3)$$

where R_{pond} = recharge from ponds (10^6 m^3); Area = water spread area of the pond (km^2); n = number of days water remains in the pond, and RF = recharge factor (ratio). Recharge from desilted ponds is estimated using a recharge factor of 1.4 mm/day (MoWR 2009). In the study area there are nearly 270 ponds with a total water spread area of 33 km^2 . Assuming water remains in these ponds for 150 days (August–December) after

Table 2 Major inflow and outflow components during the initial model period (2013–2014) and predicted scenarios for the year 2020–2021

Inflow and outflow components	Year 2013–2014	Year 2020–2021					
		Without management interventions			With management interventions		
		Scenario I (normal rain) Business-as-usual scenario	Scenario II (deficit rain) Worst-case scenario	Scenario III (surplus rain)	Scenario IV (normal rain)	Scenario V (deficit rain)	Scenario VI (surplus rain) Best-case scenario
Inflow components (mm)							
Recharge from rainfall (R_{rf})	54.1	54.1	40.4	67.3	54.1	40.4	67.3
Seepage from rivers (R_{riv})	0.3	6.2	6.2	6.9	3.9	3.8	4.0
Return flow from groundwater irrigation (R_{irr})	34.8	50.6	50.6	50.6	36.9	36.9	36.9
Recharge from different surface water sources (R_{canal})	8.4	8.4	5.1	8.4	16.3	9.1	16.3
Total inflow	97.6	119.3	102.3	133.2	111.2	90.2	124.5
Outflow components (mm)							
Draft for irrigation (D_{irr})	73.8	106.9	106.9	106.9	78.1	78.1	78.1
Draft for domestic purposes (D_{dom})	10.8	11.9	11.9	11.9	11.9	11.9	11.9
Evapotranspiration losses (ET_{gw})	11.2	3.5	2.6	4.6	5.7	4.5	7.1
Effluent seepage to rivers (D_{riv})	12.6	12.2	12.1	12.6	16.5	16.4	16.9
Total outflow	108.3	134.5	133.5	136	112.2	110.9	114
Percentage of total outflow to total inflow	111%	113%	131%	102%	101%	123%	92%

desilting, the total annual recharge is estimated to be 7.1 km^3 , which in terms of equivalent water depth (considering the entire model domain) is 0.016 mm/day . This additional recharge component is subsequently used in this study to simulate the effect of supply-side intervention on groundwater resources.

4. *Demand control.* Flood irrigation is the dominant practice in the study area, which involves huge wastage of water. As per the comprehensive mission document of National Water Mission of Govt. of India (Anon 2008), use of sprinklers and other pressure irrigation techniques may render a saving of 25–33% (average 30%) in irrigation water requirement as compared to flood irrigation. Accordingly, groundwater draft for irrigation could be reduced from the projected groundwater draft of $307 \times 10^6 \text{ m}^3$ in 2020–2021 (Ray et al. 2017a) to $224 \times 10^6 \text{ m}^3$. This reduction in draft is incorporated in the model, assuming a gradual increase in area under pressure irrigation (from 30% in 2018–2019 to 90% in 2020–2021).

While various combinations of the above stress conditions are possible, the model is run for six different scenarios and the corresponding results are discussed in the successive section.

In scenario I, groundwater draft increases as per the prediction of Ray et al. (2017a) and the area receives normal rainfall. In scenario II, groundwater draft increases as per the prediction of Ray et al. (2017a) and the year 2020–2021 is a drought year with 25% deficit in rainfall, while scenario III is assumed

to be a condition where the year 2020–2021 is a surplus rainfall year with 25% more rainfall than normal rain. Other conditions are the same as those in scenarios I and II. As such, scenarios I–III represent three different rainfall conditions without any management interventions. Further, this study assesses the impact of management interventions that include desilting of ponds, which resulted in enhanced recharge from tanks and ponds, and 90% of the irrigated area is considered to have been brought under pressure irrigation. Thus the model simulates the effect of management interventions under normal (scenario IV), 25% deficit (scenario V) and 25% surplus (scenario VI) rainfall conditions. In this set up, scenario I is the business-as-usual scenario, scenario II represents the worst-case scenario and scenario VI is the best-case scenario.

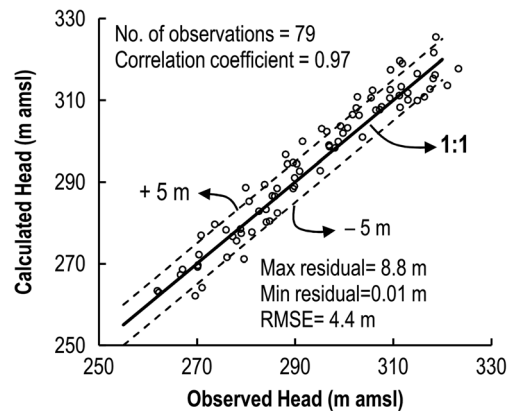
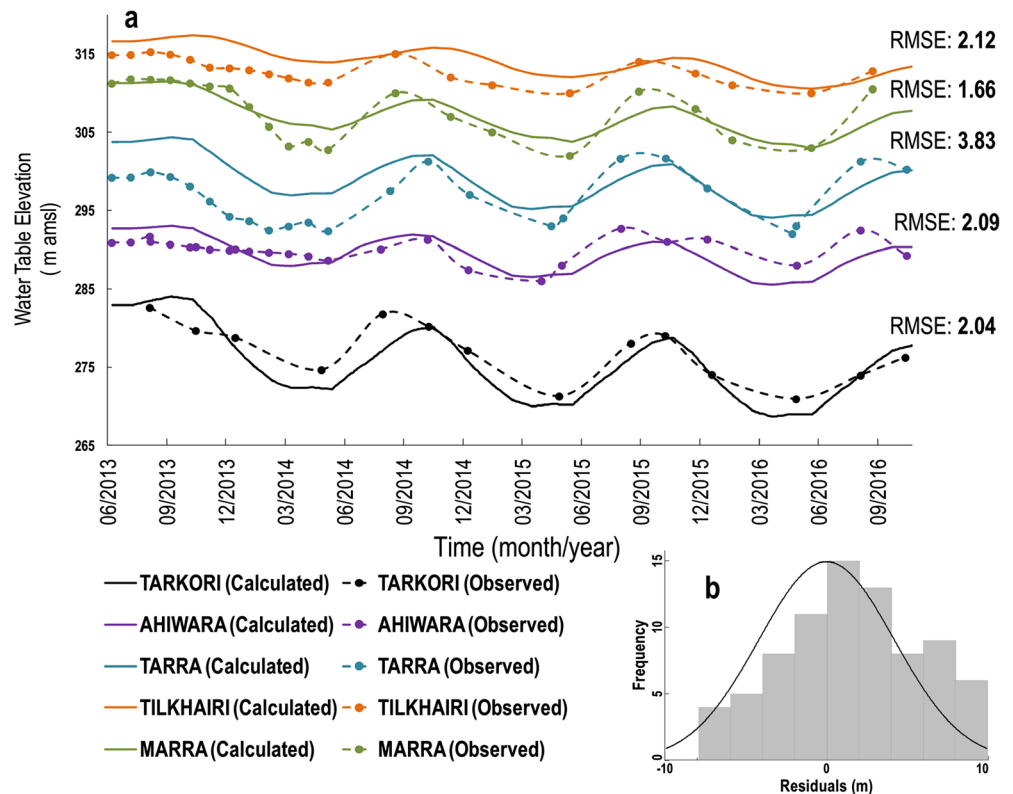


Fig. 5 Plot of observed heads vs calculated heads during steady-state run of the groundwater flow model

Fig. 6 a Calculated and observed hydrographs of water-table elevations during the transient model run. Hydrographs of Ahiwara and Tarra represent Chandi Limestone. The remaining three hydrographs of Marra, Tilkhairi and Tarkori represent Gunderdehi Shale, Charmuria Limestone and Tarenga Shale respectively. **b** Frequency distribution of residuals obtained for the initial time period during the transient model run. The solid line represents normal distribution. Locations of these selected monitoring stations are shown in Fig. 1



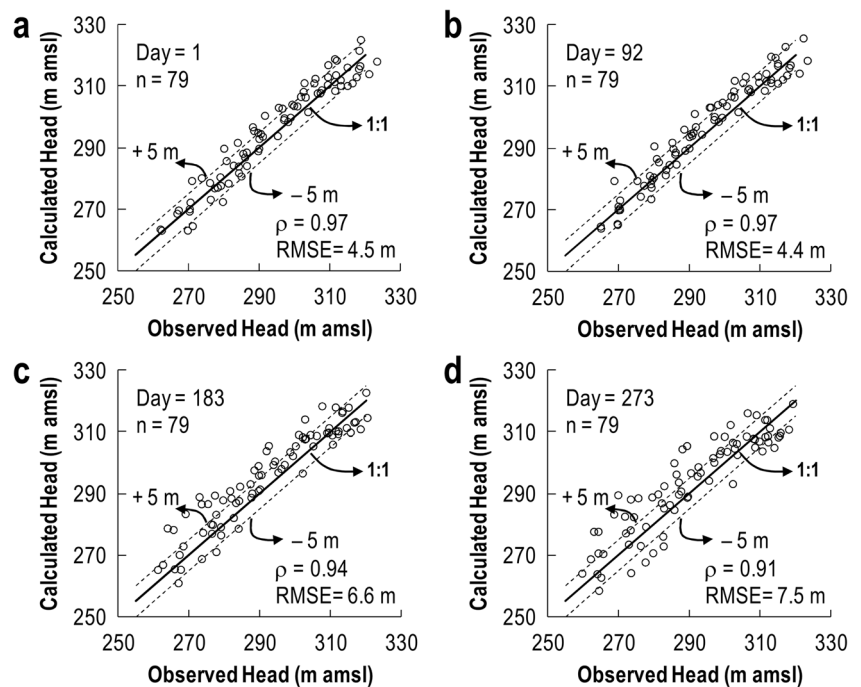
Results and discussion

Model performance

In steady-state calibration, observed water levels could be reproduced with a RMSE of 4.4 m (Fig. 5). In the transient

state model, the RMSE values for different months remain mostly within 7 m. Barring a few exceptions, the calculated heads remain within ± 4 m of the observed heads (Fig. 5). The steady-state calibration is found to be highly sensitive to hydraulic conductivity values; reduction in hydraulic conductivities resulted in an increase in calculated heads. Comparison of

Fig. 7 Calculated and observed water-table elevations at different times—**a** 1 day, **b** 92 days, **c** 183 days and **d** 273 days—during transient calibration



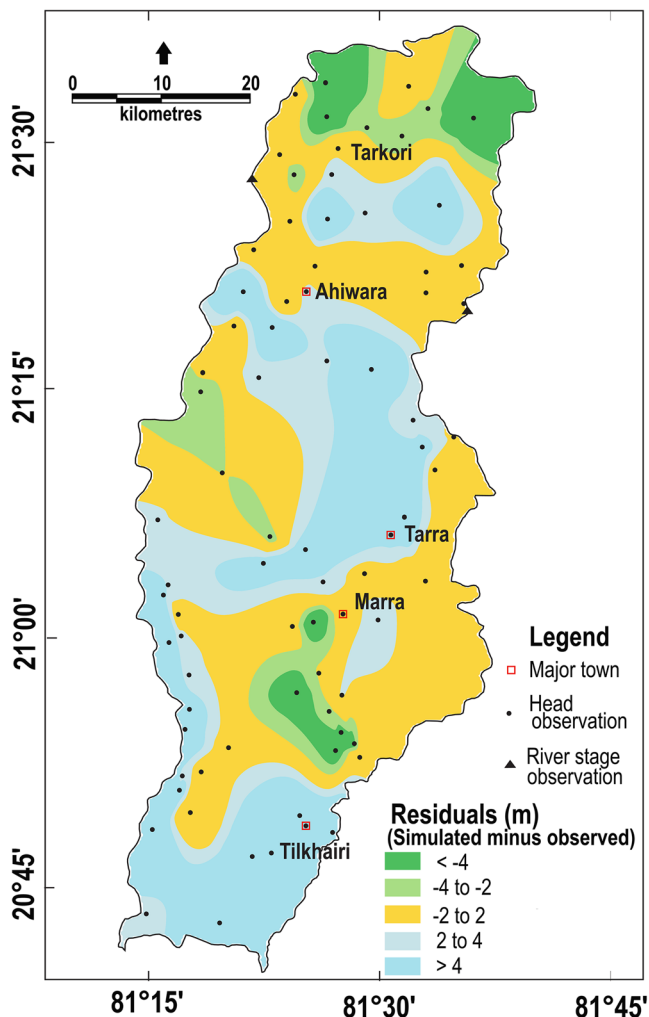


Fig. 8 Spatial distribution of residuals in water-table elevations (simulated minus observed) as obtained during the transient model run. Water-level measurement points and river-stage observation points are also shown

mass balance components estimated using Visual MODFLOW 4.2 shows that discrepancy in the estimates of input and outputs remained less than 1%. The observed groundwater flow patterns during all the periods could be reproduced. Five representative hydrographs of observed and calculated heads are shown in Fig. 6a. Amongst these, two monitoring stations represent Chandi Limestone (Ahiwara and Tarra) and the remaining three represent Gunderdehi Shale (Marra), Charmuria Limestone (Tilkhairi) and Tarenga Shale (Tarkori; Fig. 1). Sufficient numbers of water level measurements are not available for Chandarpur Sandstone and Hirri Limestone, which are of limited spatial extent. Visual comparison of observed and calculated hydrographs (Fig. 6a) shows that they match each other, reproducing the observed peaks and troughs. The RMSEs for these hydrographs (Fig. 6a) vary from 1.66 (Marra) to 3.83 (Tarra). The frequency distribution of the residuals (difference between observed and calculated heads) for

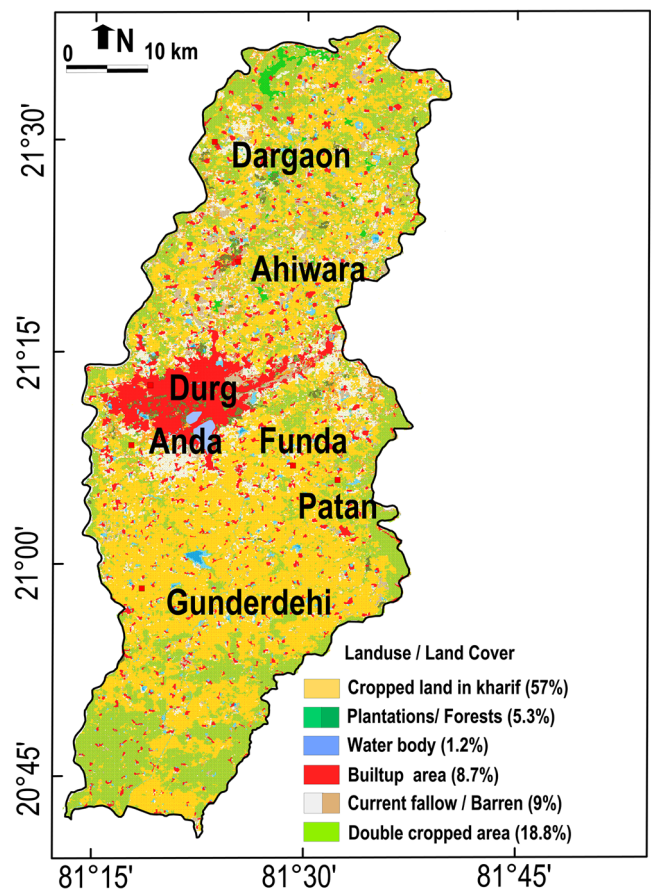


Fig. 9 Landuse/landcover map of the study area (after NRSC 2013)

the initial time of the transient run (Fig. 6b) shows that the residuals are more or less normally distributed and to a large extent (~60%) the residuals lie within ± 4 m. Comparison of observed and simulated groundwater levels during the transient run at four different time periods in 1 year is shown in Fig. 7a–d. The RMSE values during these time periods vary from 4.4 to 7.5 m with correlation coefficients ranging from 0.91 to 0.97 (Fig. 7); thus, it is evident that the calibrated model reasonably reproduces groundwater level variations over different time periods.

Analysis of the spatial distribution of residuals (Fig. 8) shows that the residuals (calculated minus observed) lie within ± 4 m over major portions (~70%) of the study area. The highest residuals are observed in the southern part of the study area, which is mostly occupied by Chamuria Limestone. A landuse map (Fig. 9) of the area (after NRSC 2013) shows that the majority of this part of the study area is cultivated twice a year (double cropped). Since irrigation is primarily based on groundwater sources, this is the area with intensive groundwater draft (Fig. 9). The errors in reproducing observed heads in the area (and elsewhere) may be attributed to uncertainties in estimation of groundwater draft for irrigation (Ray et al. 2017a). The error can also be attributed to uncertainties

Table 3 Initial estimates and calibrated values of hydraulic conductivities of different hydrostratigraphic units (*L1* and *L2* represent the first and the second model layers respectively)

Hydrostratigraphic unit	Model layer	Range of hydraulic conductivity values (m/day)			
		$K_x = K_y$		K_z	
		Initial estimate ^a	Calibrated value	Initial estimate ^b	Calibrated value
Hirri Dolomite and Tarenga Shale	L1	3–6	3.55–8.63	0.3–0.6	0.3–1.98
	L2	1.5–3	0.45–1.13	0.15–0.3	0.09–0.47
Chandi Limestone	L1	3.5–6	4–8.6	0.35–0.6	0.4–1.98
	L2	1.75–3	1.13–2.1	0.18–0.3	0.18–0.47
Gunderdehi Shale	L1	3–6	3.55–8.63	0.3–0.6	0.3–1.98
	L2	1.5–3	0.45–1.13	0.15–0.3	0.09–0.47
Charmuria Limestone	L1	6	4.85–7.25	0.6	0.36–1.28
	L2	3	0.91–2.31	0.3	0.11–0.48
Chandarpur Sandstone	L1	1	1.2	0.1	0.065
	L2	0.5	0.55	0.05	0.042

^a Generalized values based on limited pumping test data as detailed in the text

^b Initial values of K_z were taken as $0.1 \cdot K_x$

in estimation of aquifer parameters like K and S_y . More precise data on hydraulic properties and stresses could have enabled prediction of water levels with greater levels of accuracy. Notwithstanding the limitations, groundwater levels and their variations in time have been adequately represented for resource management purposes.

Aquifer parameters and recharge rates

Initial estimates and calibrated values of aquifer parameters (hydraulic conductivity and specific yield) are shown in Tables 3 and 4. Thematic maps of modelled aquifer properties are shown in Fig. 10. The horizontal hydraulic conductivity ($K_x = K_y$) values of layer one (up to 100 m depth) range from 1.2 m/day in Chandarpur sandstone to 8.6 m/day in parts of Chandi, Hirri and Gunderdehi Formations. Gleeson et al. (2011) provided a review of permeability (k) values based on calibrated models where the permeability values of carbonates ranged from 1×10^{-16} to 1×10^{-8} m². The hydraulic

conductivity (K_x and K_y in m/day) values of Precambrian carbonates of Chhattisgarh Supergroup reported in this paper range from 2.3 to 8.6 m/day, which in permeability (k) terms is equivalent to 2.7×10^{-12} to 10.2×10^{-12} m² and as such lie within the typical range of 1×10^{-16} to 1×10^{-8} m² for carbonates (Gleeson et al. 2011). These reported ranges of horizontal hydraulic conductivity values are also comparable to those adopted for flow modeling in carbonate aquifers of various ages in many previous studies (Gallegos et al. 2013; Gonzalez-Herrera et al. 2002; Romanazzi et al. 2015).

However, the range of horizontal hydraulic conductivity values (3.6 to 8.6 m/day, which is equivalent to 1×10^{-12} to 7×10^{-12} m²) obtained for Gunderdehi Shale and Tarenga Shale are significantly higher than the typical range of values (1×10^{-20} to 1×10^{-14} m²) obtained for ‘fine-grained sedimentary’ formations reported by Gleeson et al. (2011). In fact, hydraulic conductivity values of these shale units are rather better comparable to those of the limestone units. This is primarily because both Tarenga Shale and Gunderdehi Shale are calcareous shale units with intercalations of sandstone and limestone (Das et al. 1992; Mukherjee et al. 2014). Patranabis-Deb and Chaudhuri (2002) also reported stromatolitic limestone within the Gunderdehi Formation from the Baradwar subbasin. Though the shale units in the study area have lower groundwater potential than the carbonates (Chandarpur Limestone, Charmuria Limestone and Hirri Dolomite), they often form good aquifers. Instances of high sulphate in groundwater have been reported from these shale units, which can be attributed to presence of gypsum veins (Mukherjee et al. 2014). Ray et al. (2017b), based on a study involving groundwater hydrochemistry, had shown that dissolution of carbonates and sulphates

Table 4 Initial estimates and calibrated values of specific yield (S_y) of different hydrostratigraphic units

Hydrostratigraphic unit	Range of S_y values (%)	
	Initial estimate ^a	Calibrated value
Hirri Dolomite and Tarenga Shale	0.04	0.0033–0.0305
Chandi Limestone	0.04	0.0042–0.0305
Gunderdehi Shale	0.0038	0.0033–0.0305
Charmuria Limestone	0.04	0.019
Chandarpur Sandstone	0.0038	0.0021

^a Based on dry season water balance study as reported by Ray et al. (2014)

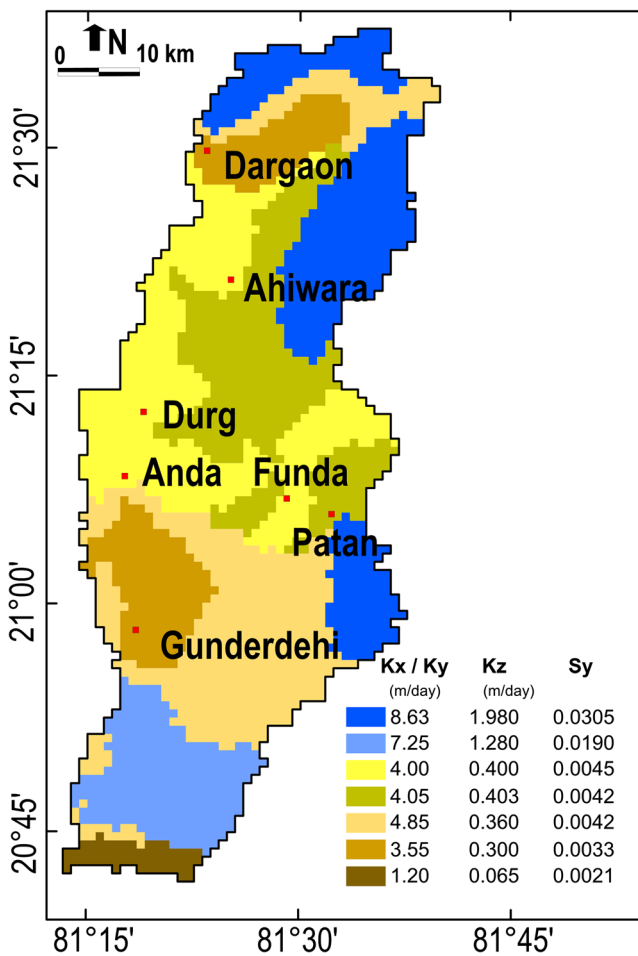


Fig. 10 Spatial distribution of hydraulic conductivity ($K_x/K_y, K_z$) and specific yield (S_y) values as derived from the calibrated model

are predominant processes even in the shale units. Consequently, these processes resulted in the formation of solution cavities that contribute significantly towards increase in the values of hydraulic conductivity. Vertical hydraulic conductivity (K_z) values as obtained from the auto-calibrated model range from 0.042 (m/day) in Chandarpur Sandstone to 1.98 (m/day) in parts of Tarenga Shale, Chandi Limestone and Gunderdehi Shale (Table 3 and Fig. 10). Specific yield (S_y) values obtained from the calibrated model also vary over a wide range, starting from 0.002 in Chandarpur Sandstone to 0.03 in parts of Tarenga Shale, Chandi Limestone and Gunderdehi Shale (Table 4). Spatial distribution of S_y is shown in Fig. 10. Annual rainfall recharge rates are 3–4.8% of rainfall in areas underlain by Chandarpur Sandstone and Charmuria Limestone respectively. Even within the same hydrostratigraphic unit, there is noticeable variation in recharge rates in different seasons. During the monsoon period the recharge rates in different hydrostratigraphic units vary from 3% (Gunderdehi/Chandi) to 4.8% (Chandi/Charmuria), whereas during

the nonmonsoon period the values vary from 5% (Gunderdehi/Chandi) to 8% (Chandi/Charmuria).

Regional groundwater balance

Major water balance components considered in the present model are discussed in section ‘Sources and sinks’. Comparison of the input and output components under different scenarios is given in Table 2. For ease of comparison, the source and sink terms in the table are expressed in equivalent water depth (in mm) by dividing the volume by the geographical area (i.e. 2,867 km²). The sum of all the input components during 2013–2014 is 97.6 mm ($279 \times 10^6 \text{ m}^3/2,867 \text{ km}^2$), of which R_{rf} , R_{canal} and R_{irr} account for around 55, 9 and 36%, respectively. Seepage from rivers (R_{riv}) is estimated to be negligible (less than 1%). Similarly, out of the gross outflow of 108.3 mm ($309 \times 10^6 \text{ m}^3/2,867 \text{ km}^2$), D_{irr} and D_{dom} account for 68 and 10% respectively, while ET_{gw} and D_{riv} account for ~10% each. Recharge from rainfall and draft for irrigation are the predominant inflow and outflow components respectively. Return flow from irrigation (R_{irr}) contributes to a significant portion (~25% in scenario III to ~50% in scenario II) of the recharge. Rivers in the study area are mostly effluent in nature (fed by groundwater) and contribute negligibly to groundwater recharge. More than 20% of the annual recharge is lost to evapotranspiration (ET_{gw}) and baseflow to the rivers (D_{riv}). In its entirety, total outflow ($D_{irr} + D_{dom} + ET_{gw} + D_{riv}$) exceeds total inflow ($R_{rf} + R_{canal} + R_{irr} + R_{riv}$) by ~10% during the initial year of study (2013–2014), thereby indicating overexploited conditions.

Comparison of monthly averages of total inflow and outflow components for the year 2013–2014 (initial model period; Fig. 11) reveal that recharge from rainfall is the highest

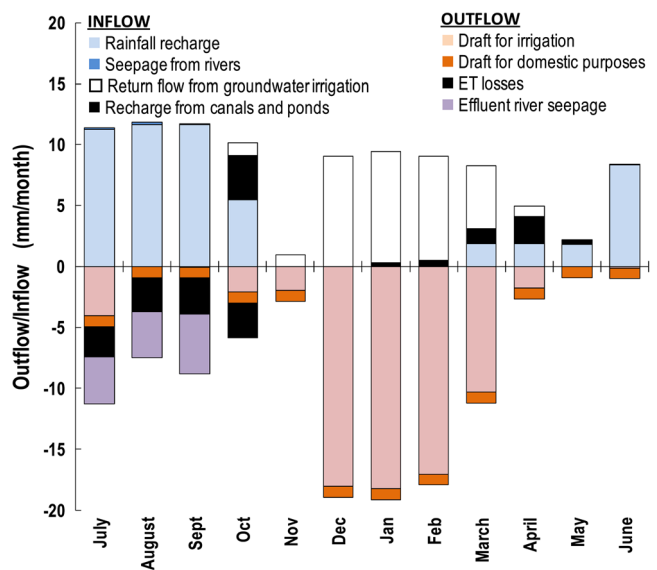


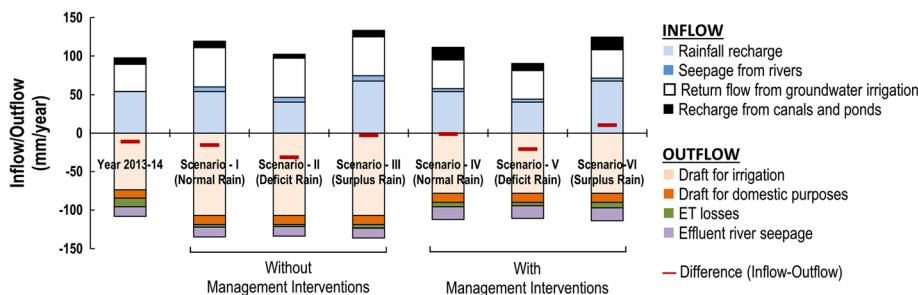
Fig. 11 Monthly total inflow and outflow components (expressed in mm) for the initial model year (2013–2014)

during the monsoon months (July, August and September). Inflows in the months of December, January, February and March are attributed dominantly to return flow from groundwater irrigation. Groundwater draft for irrigation is the highest during December, January and February, which are the major cropping months. High outflows during the months of July, August and September, as shown in Fig. 11, represent effluent seepage to the rivers.

Response of the aquifer system to projected changes in stress conditions

As described in the previous sections, model simulations are performed for six different scenarios that assumed probable changes in stress (inflow and outflow components) for the year 2020–2021. Inflow and outflow components during the initial model year (2013–2014) and in different projected scenarios are compared in Table 2 and Fig. 12. Except for scenario VI, total annual outflow exceeds total annual inflow in all cases including the initial model year (Table 2 and Fig. 12). In the simulations in which groundwater management interventions have not been implemented, total outflow exceeds total inflow by around 2% (131%) in the surplus (deficit) rainfall scenario (Table 2 and Fig. 12). Comparison of water balance components in the scenarios (scenarios IV–VI), in which management interventions are included, reveal that in scenario IV total outflow does not exceed total inflow notably. With demand side interventions, such as pressure irrigation in 90% of the irrigated area, groundwater extraction in 2020–2021 is estimated to come down almost to the level of extraction in the initial model year (2013–2014). The results show that with the suggested management interventions, even during a normal rainfall year, groundwater draft is only marginally higher than the annual recharge (Fig. 12; Table 2); however, under a deficit rainfall scenario, groundwater draft is found to exceed annual recharge by about 10% (Fig. 12; Table 2). It is important to note that, while recharge augmentation measures, as simulated here, contribute to only 10 mm of additional recharge (Table 2), demand control measures have the potential to reduce groundwater draft by ~28 mm (106.91–78.13). These estimates indicate that demand control measures are more effective than recharge augmentation measures.

Fig. 12 Comparison of different annual inflow and outflow components in the initial model year (2013–2014) and in the year 2020–2021 under six different scenarios. Inflow and outflow components are given in Table 2



Spatial variations in groundwater level for the year 2020–2021, in comparison to those in the year 2013–2014, for different scenarios are shown in Fig. 13a–f. While Fig. 13a–c depicts water-table variations in normal, deficit and surplus rainfall conditions without management interventions, Fig. 13d–f depicts those with management interventions. In general, groundwater levels in the year 2020–2021 show prominent decline in scenarios I–III when compared to those in the year 2013–2014 (Fig. 13). In a normal rainfall year (scenario I), up to 15 m decline in water level is observed (Fig. 13a). Under a scenario where management interventions are not implemented, the water table shows prominent decline even during surplus rainfall year (Fig. 13c). On the other hand, with proper management interventions, even in a normal rainfall year, water level in many parts of the study area show significant rise in comparison to that in 2013–2014 (Fig. 13d).

In scenario VI (the best-case scenario), water levels in nearly one third of the study area show rise from 2013 to 2014 levels (Fig. 13f), although with a low magnitude. Years 2013–2014 through 2019–2020, irrespective of the scenarios, represent overexploited conditions where total outflows exceed total inflows and hence groundwater level continues to decline over this period. In the year 2020–2021 overexploitation is predicted to worsen significantly in a business-as-usual scenario, whereas with proper management interventions, it is shown that overexploitation can be contained. In a surplus rainfall year (scenario VI) groundwater levels even show rise in comparison to present day water levels. This indicates that groundwater levels are expected to completely recover (or even rise) if such favourable conditions could be maintained over the years.

Limitations

One of the major limitations for developing a regional groundwater flow model is the lack of sufficient ground-based data (Zhou and Li 2011), especially in the context of the Indian subcontinent. Likewise, crucial aquifer properties like K and S_y incorporated in the model are generally based on limited field observations; thus, incorporation of more site-specific data is bound to improve the model simulations significantly. Moreover, the rivers and surface water flows are inadequately represented in the model. An integrated surface-water/

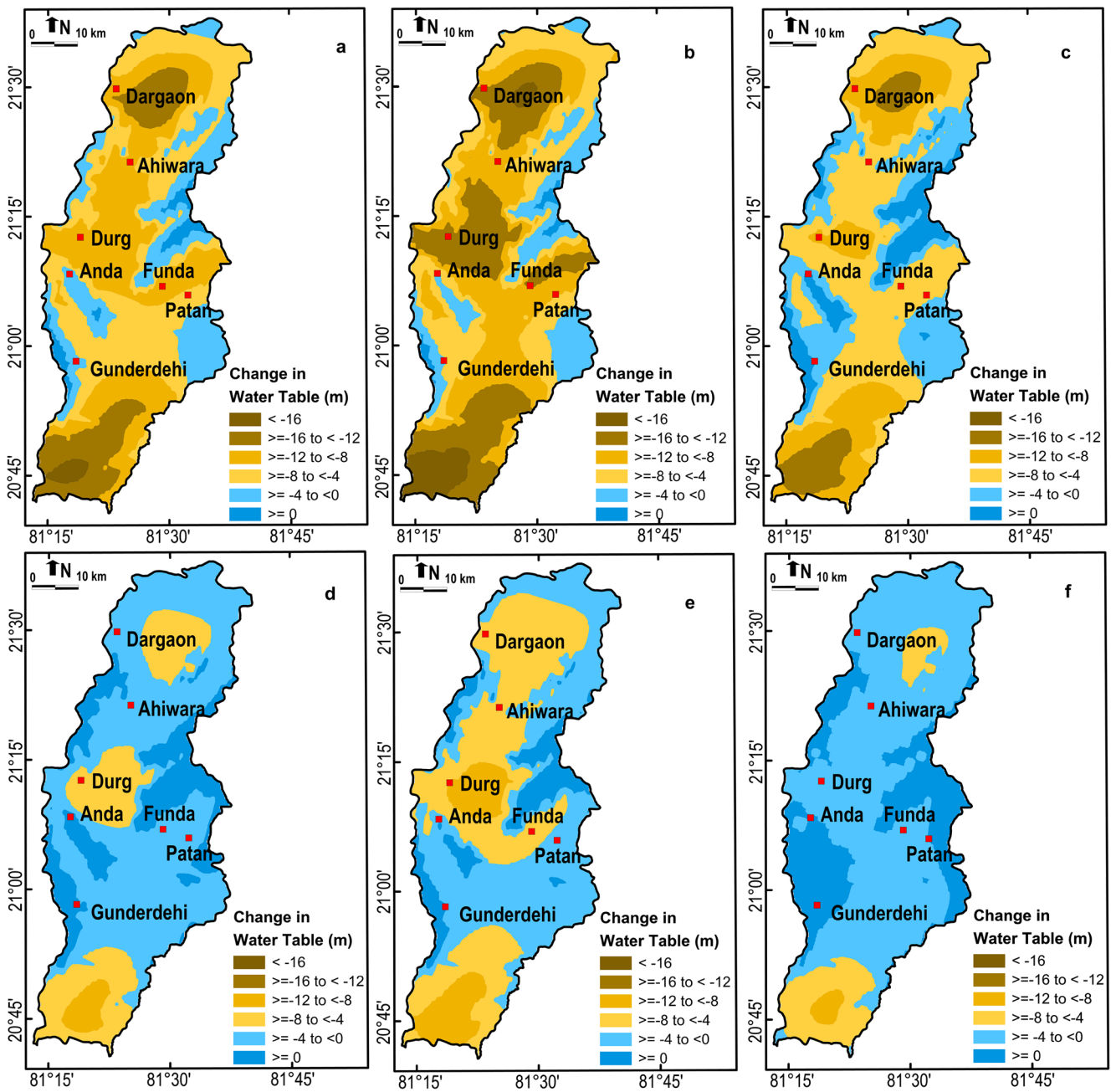


Fig. 13 Projected decline in water level in June 2021 (year 2020–2021) with reference to June 2014 (year 2013–2014) under six different scenarios—**a** scenario I: normal rainfall without management interventions, **b** scenario II: deficit rainfall without management interventions, **c** scenario III: surplus

rainfall without management interventions, **d** scenario IV: normal rainfall along with management interventions, **e** scenario V: deficit rainfall along with management interventions, **f** scenario VI: surplus rainfall along with management interventions

groundwater model may provide better insights into the dynamics of groundwater in the area. Also note that, in this study, model predictions, till the year 2020–2021, are based on calibrations made only over a limited period of three years starting from 2013–2014. Even though an extended calibration period might have improved the quality of simulations, the comprehensive groundwater draft estimates required to do so are only available for the years 2014 onwards. Further, an

equivalent porous media approach is implemented to represent the hydrostratigraphic units in the area. Perhaps a detailed model incorporating the properties of fractures/caverns, instead of assuming equivalent porous media, could have improved the accuracy of the model. However, here also, the data required for incorporating such finer details into the flow model are practically impossible to obtain for the study area. Furthermore, only the rainfall recharge estimate used in this study is based on area

specific observations (chloride mass balance), whereas other recharge components such as seepage from canal water, return flow from irrigation, and seepage from ponds and standing water bodies, are based on predefined norms (MoWR 2009) only. However, it is important to note that despite its limitations, the model developed here has demonstrated its capability to aid in the pursuit of actionable information on the dynamics and sustainability of groundwater resources and to quantify different water budget components at relevant spatial scales.

Conclusions

The Seonath-Kharun interfluvial area is one of the most water-stressed regions in the Chhattisgarh State of India. Nearly 1.8 million people living in the area are almost entirely dependent on groundwater for drinking as well as irrigation purposes. Moreover, the study area represents the complexities of Precambrian sedimentary terrains and other hard-rock areas in India, which cover nearly 70% of the country's geographical area. Over a period of eight water years (2013–2014 to 2020–2021), irrigation and domestic drafts of groundwater are predicted to increase by 44 and 10% respectively. Groundwater development at this rate may be unsustainable and is therefore likely to threaten the livelihood of the populace. Although groundwater management is an immediate requirement, sufficient data, in appropriate scale, are not available to make informed management decisions. Further, the study area, which is comprised of Precambrian sedimentary rocks with the predominance of fractures, pose additional challenges to understand groundwater flow dynamics and quantify the different components of hydrologic balance. This study provides an assessment of groundwater input and output components, suggests feasible management interventions and predicts the response of the groundwater system to these interventions, using an equivalent porous medium (EPM)-based groundwater flow model.

This study also demonstrates that the groundwater flow model based on the EPM approach can be effectively used in data-scarce areas for assessing and predicting groundwater dynamics. In an earlier assessment of groundwater resources in India (MoWR 2009), only 5–10% of annual recharge was considered to account for natural losses like baseflow, while no separate assessment of evapotranspiration losses from groundwater was reported. Instead, the present study shows that evapotranspiration and effluent seepage to rivers can be as high as 20% of the total annual recharge. This study is also consistent with the recently revised methodology for groundwater resource assessment of India (CGWB 2017b), which recommends separate assessments of all water balance components including evapotranspiration and baseflow; hence,

the methodology adopted in the present study can be applied for such assessments. Similarly, aquifer parameters (K and S_y) and rainfall recharge rates as derived from the calibrated model are significantly different from the recommended norms for estimation of groundwater resources in India (MoWR 2009) and can therefore be used for refining the existing norms and reported estimates.

In this study the groundwater flow model is run for a period of 8 years starting from the water year 2013–2014 (July 2013 to June 2014). The model simulations represent response of the local groundwater system to changing stress conditions, as assessed under six different scenarios. Results from this analysis show that during the initial water year (2013–2014) the total annual outflow exceeds annual input by 11%, and this deficit increases to 13 and 31% for the 2020–2021 period under business-as-usual and worst-case scenarios (drought condition) respectively (Table 2). This underscores the necessity of suitable management strategies to augment the resources and/or restrict rampant groundwater extraction in order to ensure better sustainability. There are approximately 270 waterbodies in the study area, which when desilted can act as effective recharge structures and can contribute ~10 mm/year of additional recharge. Flood irrigation is the predominant practice in the area, and it is observed that by adopting pressure irrigation techniques (sprinklers and drip), annual draft for irrigation in the year 2020–2021 can be brought down from 106.91 to 78.13 mm. Model simulations also reveal that demand control measures like reduction of groundwater draft through adoption of efficient irrigation practices can be more effective than supply side interventions (augmenting groundwater recharge), while adopting both can even help contain serious over-exploitation issues. In the best-case scenario, with additional recharge from waterbodies, reduced draft (because of the adoption of pressure irrigation techniques), and surplus rainfall (25% more rainfall than the normal year), the total outflow for the year 2020–2021 could be restricted to ~90% of the annual inflow. Further, comparison of groundwater level variations under different rainfall scenarios along with and without management interventions, reveal that management interventions have more pronounced impact than the rainfall variations.

Availability of more input data based on site-specific tests, and consideration of longer periods of observed data for calibration would certainly provide better insights into the regional groundwater dynamics and improve the model's predictive capabilities. However, in spite of the known limitations, the current study provides the best available assessment of existing and future groundwater scenarios in the study area, which can be key to providing actionable recommendations at local scale. This study also provides newer insights and refined assessment of aquifer parameters and recharge rates,

which can be used for groundwater assessment and management in similar terrains.

Acknowledgements Groundwater level and borehole litholog data collected and archived by Central Ground Water Board (CGWB), Department of Water Resources, River Development and Ganga Rejuvenation, Ministry of Jal Shakti have been used in the paper for which the authors are thankful to the Chairman, CGWB. River flow, river-stage and canal data were obtained from water resources department of Govt. of Chhattisgarh, for which the authors thank the concerned authorities, especially Shri Sonkusale, Shri Shukla and Shri Chaudhury. Infrastructure facilities including necessary software provided by CGWB and IIT (ISM) Dhanbad in pursuing the study are thankfully acknowledged. Opinions contained in the paper are those of the authors and they do not necessarily represent the opinions of the organisations they are affiliated to. The authors are grateful to the reviewers for their thorough scrutiny of the manuscript and valuable suggestions, which improved the quality significantly. The authors would also like to thank the technical editor for her helpful instruction and meticulous corrections.

References

- Abbo H, Shavit U, Markel D, Rimmel A (2003) A numerical study on the influence of fractured regions on lake/groundwater interaction: the Lake Kinneret (Sea of Galilee) case. *J Hydrol* 283:225–243. [https://doi.org/10.1016/S0022-1694\(03\)00273-7](https://doi.org/10.1016/S0022-1694(03)00273-7)
- Ahmad I, Umar R (2009) Groundwater flow modelling of Yamuna-Krishni intersection, a part of central Ganga plain, Uttar Pradesh. *J Earth Syst Sci* 118(5):507–523
- Ahmed S, Engerrand C, Sreedevi PD, Kumar D, Subrahmanyam K, Ledoux E, Marsily G (2003) Geostatistics, aquifer modeling and artificial recharge, scientific report: volume 3, indo-French collaborative project (2003-1). Technical report NGRI-2003-GW-41, NGRI, Hyderabad, India
- Alam F, Umar R (2013) Groundwater flow modelling of Hindon-Yamuna interfluvial region, western Uttar Pradesh. *J Geol Soc India* 82:80–90. <https://doi.org/10.1007/s12594-013-0113-8>
- Anderson MP, Woessner WW (1992) Applied groundwater modeling, simulation of flow and advective transport. Academic, New York
- Anon (2008) Comprehensive mission document, vol 2. National Water Mission under the National Action Plan on Climate Change, Ministry of Water Resources, Govt. of India, 471 pp. <http://wrmin.nic.in/writeraddata/nwm28756944786.pdf>. Accessed 17 November 2017
- CGWB (2006a) State report: hydrogeology of Chhattisgarh. Central Ground Water Board, North Central Chhattisgarh Region (NCCR), Raipur, India, 184 pp
- CGWB (2006b) Dynamic ground water resources of India (as on March 2004). Central Ground Water Board, Ministry of Water Resources, Govt. of India. <http://cgwb.gov.in/Documents/Dynamic-GW-Resources-2004.pdf>. Accessed 17 November 2017
- CGWB (2011) Dynamic ground water resources of India (as on March 2009). Central Ground Water Board, Ministry of Water Resources, Govt. of India. <http://cgwb.gov.in/Documents/Dynamic-GW-Resources-2009.pdf>. Accessed 17 November 2017
- CGWB (2012) Aquifer systems of Chhattisgarh, North Central Chhattisgarh Region. Central Ground Water Board, Ministry of Water Resources, Govt. of India. <http://cgwb.gov.in/AQM/Chhattisgarh.pdf>. Accessed 17 November 2017
- CGWB (2013) Master plan for artificial recharge to ground water in India. Central Ground Water Board, Ministry of Water Resources, Govt. of India. Accessed 17 November 2017
- CGWB (2014) Dynamic ground water resources of India (as of 31st March 2011). Central Ground Water Board, Ministry of Water Resources, Govt. of India. <http://cgwb.gov.in/Documents/Dynamic-GW-Resources-2011.pdf>. Accessed 17 November 2017
- CGWB (2017a) Dynamic ground water resources of India (as of 31st March 2013). Central Ground Water Board, Ministry of Water Resources, Government of India. <http://cgwb.gov.in/Documents/Dynamic-GW-Resources-2011.pdf>. Accessed 17 November 2017
- CGWB (2017b) Report of the ground water resource estimation committee (GEC 2015): methodology. Ministry of Water Resources, River Development and Ganga rejuvenation, Govt. of India. http://cgwb.gov.in/Documents/GEC2015_Report_Final%2030.10.2017.pdf. Accessed 17 November 2017
- CGWB (2019) National compilation on dynamic ground water resources of India 2017. Central Ground Water Board, Department of Water Resources, River Development and Ganga Rejuvenation, Ministry of Jal Shakti, Government of India. <http://cgwb.gov.in/GWAssessment/GWRA-2017-National-Compilation.pdf>. Accessed 28 February 2020
- Chandraprakash (2017) Studies on drought in Kharun sub basin for supplemental irrigation planning of kharif crops. MSc Thesis, Indira Gandhi Krishi Vishwavidyalaya, Raipur, India, 120 pp. www.krishikosh.egranth.ac.in/bitstream/1/5810035227/1/thesis.pdf. Accessed 17 November 2017
- Chatterjee R, Ray RK (2016) A proposed new approach for groundwater resources assessment in India. *J Geol Soc India* 88(3):357–365. <https://doi.org/10.1007/s12594-016-0498-2>
- Das DP, Kundu A, Dutta DR, Kumaran K, Ramamurthy S, Thanavelu C, Ragaiya V (1992) Lithostratigraphy and sedimentation of Chhattisgarh basin. *Indian Mineral* 46(3–4):271–288
- DWAF (2006) Methodology for groundwater quantification. GRA II Task: 1A, 1BC, 1D. Department of Water Affairs and Forestry, Pretoria, South Africa
- Famiglietti JS (2014) The global groundwater crisis. *Nat Clim Chang* 4: 945
- FAO (2016) AQUASTAT main database, food and agriculture organization of the United Nations (FAO). <http://www.fao.org/nr/water/aquastat/data/query/index.html?lang=en>. Accessed Feb 2020
- Ford DC, Williams PW (2007) Karst hydrogeology and geomorphology. Wiley, Chichester, UK
- Gallegos JJ, Hu BX, Davis H (2013) Simulating flow in karst at laboratory and sub-regional scales using MODFLOW-CFP. *Hydrogeol J* 21:1749–1760. <https://doi.org/10.1007/s10040-013-1046-4>
- Gleeson T, Smith L, Moosdorf N, Hartman J, Dürr Manning AH, van Beek PH, Jellinek AM (2011) Mapping permeability over the surface of the earth. *Geophys Res Lett* 46:L02401. <https://doi.org/10.1029/2010GL045565>
- Gonzalez-Herrera R, Sanchez-y-Pinto I, Gamboa-Vargas J (2002) Groundwater-flow modeling in Yucatan karstic aquifer, Mexico. *Hydrogeol J* 10:539–552
- Gupta AK, Tyagi P, Sehgal VK (2011) Drought disaster challenges and mitigation in India: strategic appraisal. *Curr Sci* 100(12):1795–1806. <http://www.currentscience.ac.in/volumes/100/12/1795.pdf>. Accessed 17 November 2017
- Harbaugh AW, Banta ER, Hill MC, McDonald MG (2000) MODFLOW 2000, the US Geological Survey modular groundwater model: user guide to modularisation concepts and groundwater flow process. US Geol Surv Open-File Rep 00-92, 121 pp
- Huntoon PW (1994) Is it appropriate to apply porous media groundwater circulation models to karstic aquifers? In: El-Kadi AI (ed)

- Groundwater models for resources analysis and management. Pacific Northwest/Oceania Conference, Honolulu, HI, pp 339–358
- IMD (2020) Glossary. India Meteorological Department (IMD), Pune. <http://www.imdpune.gov.in/Weather/Reports/glossary.pdf>. Accessed 11 January 2020
- Kaehler CA, Hsieh PA (1994) Hydraulic properties of a fractured-rock aquifer, Lee Valley, San Diego County, California. US Geol Surv Water Suppl Pap 2394, 64 pp
- Kansal ML, Chandniha SK, Tyagi A (2015) Distance based water sustainability assessment using SPI for the state of Chhattisgarh in India. In: Karvazy PE, Webster VL (ed) World Environmental and Water Resources Congress 2015: Floods, Droughts, and Ecosystems, Austin, TX, May 2015
- Khare MC (1981) Sedimentological and hydrogeological studies of parts of Durg and Raipur districts, M.P., India. PhD Thesis, University of Roorkee, India, 351 pp
- Kumar N (2014) Impacts of climate change and land-use change on the water resources of the Upper Kharun Catchment, Chhattisgarh, India. PhD Thesis, Rheinischen Friedrich-Wilhelms-Universität zu Bonn, Germany. http://hss.ulb.uni-bonn.de/diss_online. Cited. Accessed 18 June 2017
- Kumar T, Gautam AK (2014) Appraising the accuracy of GIS based multicriteria decision making technique for delineation of groundwater potential zones. *Water Resour Manag* 28(13):4449–4466
- Kushwaha RK, Pandit MK, Goyal R (2009) MODFLOW based groundwater resource evaluation and prediction in Mendha sub-basin, NE Rajasthan. *J Geol Soc India* 74:449–458
- Langevin CD (2003) Simulation of submarine ground water discharge to a marine estuary: Biscayne Bay, Florida. *Groundwater* 41(6):758–771
- MoWR (2009) Ground water resource estimation methodology. Report, Ground Water Resource Estimation Committee, Ministry of Water Resources, Govt. of India, 107 pp. <http://cgwb.gov.in/documents/gec97.pdf>. Accessed 17 November 2017
- Mukherjee A, Fryar AE, Howell PD (2007) Regional hydrostratigraphy and groundwater flow modeling in the arsenic-affected areas of the western Bengal basin, West Bengal. *Hydrogeol J* 15(7):1397–1418. <https://doi.org/10.1007/s10040-007-0208-7>
- Mukherjee A, Ray RK, Tewari D, Ingle VK, Sahoo BK, Khan MWY (2014) Revisiting the stratigraphy of the Mesoproterozoic Chhattisgarh Supergroup, Bastar craton, India based on subsurface lithoinformation. *J Earth Syst Sci* 123(3):617–632
- Narasimhan TN (2008) A note on India's water budget and evapotranspiration. *J Earth Syst Sci* 117(3):237–240
- Neuman SP (1987) Stochastic continuum representation of fractured rock permeability as an alternative to the REV and fracture network concepts. In: Custodio E, Gurgui A, Lobo-Ferreira JP (eds) NATO advanced workshop on advances in analytical and numerical groundwater flow and quality modelling. In: NATO ASI Series C: mathematical and physical sciences, vol 224. Reidel, Dordrecht, The Netherlands, pp 331–362
- NRC (1996) Rock fractures and fluid flow: contemporary understanding and applications. USA National Research Council (NRC), National Academic Press, Washington, DC, 551 pp
- NRSC (2013) Thematic map of land use and land cover (250K) for the year 2012–13. <http://bhuvan.nrsc.gov.in/gis/thematic/index.php>. Accessed February 2020
- Panagopoulos G (2012) Application of MODFLOW for simulating groundwater flow in the Trifilia karst aquifer, Greece. *Environ Earth Sci* 67:1877–1889. <https://doi.org/10.1007/s12665-012-1630-2>
- Pankow JF, Johnson RL, Hewetson JP, Cherry JA (1986) An evaluation of contaminant migration patterns at two waste disposal sites on fractured porous media in terms of the equivalent porous medium (EPM) model. *J Contaminant Hydrol* 1:65–76
- Patranabis-Deb S, Chaudhuri AK (2002) Stratigraphic architecture of the Proterozoic succession in the eastern Chhattisgarh Basin, India: tectonic implications. *Sediment Geol* 147:105–125
- Quinlan JF, Davies GJ, Jones SW, Huntoon PW (1996) The applicability of numerical models to adequately characterize groundwater flow in karstic and other triple-porosity aquifers. In: Ritchy JD, Rumbaugh JO (eds) Subsurface fluid-flow (ground-water and vadose zone) Modeling. ASTM STP 1288, American Society for Testing and Materials, West Conshohocken, PA, pp 114–133
- Ray RK, Mukherjee A, Mukherjee R (2014) Estimation of specific yields of individual litho-units in a terrain with multiple litho-units: a water balance approach. *J Geol Soc India* 84(2):221–225. <https://doi.org/10.1007/s12594-014-0126-y>
- Ray RK, Syed TH, Saha D, Sarkar BC, Patre AK (2017a) Assessment of village-wise groundwater draft for irrigation: a field-based study in hard-rock aquifers of central India. *Hydrogeol J* 25(8):2513–2525. <https://doi.org/10.1007/s10040-017-1625-x>
- Ray RK, Syed TH, Saha D, Sarkar BC, Reddy DV (2017b) Recharge mechanism and processes controlling groundwater chemistry in a Precambrian sedimentary terrain: a case study from central India. *Environ Earth Sci* 76:136. <https://doi.org/10.1007/s12665-017-6435-x>
- Rhode MM, Edmunds WM, Freyberg D, Sharma OP, Sharma A (2015) Estimating aquifer recharge in fractured hard rock: analysis of the methodological challenges and application to obtain a water balance (Jaisamand Lake Basin, India). *Hydrogeol J* 23:1573–1586. <https://doi.org/10.1007/s10040-015-1291-9>
- Romanazzi A, Gentile F, Polemio M (2015) Modelling and management of a Mediterranean karstic coastal aquifer under the effects of seawater intrusion and climate change. *Environ Earth Sci* 74(1):115–128. <https://doi.org/10.1007/s12665-015-4423-6>
- Sahoo S, Jha MK (2017) Numerical groundwater-flow modeling to evaluate potential effects of pumping and recharge: implications for sustainable groundwater management in the Mahanadi delta region, India. *Hydrogeol J* 25(2489):2489–2511. <https://doi.org/10.1007/s10040-017-1610-4>
- Scanlon BR, Mace RE, Barrett ME, Smith B (2003) Can we simulate regional groundwater flow in a karst system using equivalent porous media models? Case study, Barton Springs Edwards aquifer, USA. *J Hydrol* 276:137–158. [https://doi.org/10.1016/S0022-1694\(03\)00064-7](https://doi.org/10.1016/S0022-1694(03)00064-7)
- Schwarz FW, Smith L (1988) A continuum approach for modelling mass transport in fractured media. *Water Resour Res* 24(8):1360–1372
- Shah N, Nachabe M, Ross M (2007) Extinction depth and evapotranspiration from ground water under selected land covers. *Groundwater* 45(3):329–338. <https://doi.org/10.1111/j.174-6584.2007.00302.x>
- Sikdar PK, Chakraborty S (2017) Numerical modelling of groundwater flow to understand the impacts of pumping on arsenic migration in the aquifer of North Bengal plain. *J Earth Syst Sci* 126:29. <https://doi.org/10.1007/s12040-017-0799-x>
- Singhal BBS, Gupta RP (1999) Applied hydrogeology of fractured rocks. Kluwer, Dordrecht, The Netherlands, 375 pp
- Smith L, Schwarz FW (1984) An analysis of influence of fracture geometry on mass transport in fractured media. *Water Resour Res* 20(9):1241–1255
- Surinaidu L, Gurunadha S, Rames G (2013) Assessment of groundwater inflows into Kuteshwar limestone mines through flow modelling study, Madhya Pradesh, India. *Arab J Geosci* 6:1153–1161. <https://doi.org/10.1007/s12517-011-0421-5>
- Surinaidu L, Gurunadha Rao VVS, Srinivasa Rao N, Srinu S (2014) Hydrogeological and groundwater modeling studies to estimate the

- groundwater inflows into the coal mines at different mine development stages using MODFLOW, Andhra Pradesh, India. *Water Resour Indust* 7-8:49–65. <https://doi.org/10.1016/j.wri.2014.10.002>
- SWS (2010) *Dynamic Groundwater Flow and Contaminant Transport Modeling Software: user's manual*. Schlumberger Water Services, Kitchener, ON, 676 pp
- Thangarajan M (1999) Numerical simulation of groundwater flow regime in a weathered hard rock aquifer. *J Geol Soc India* 53(5):561–570
- Walton WC (1970) *Groundwater resource evaluation*. McGraw Hill, New York, 664 pp
- White WN (1932) A method of estimating ground water supplies based on discharge by plants and evaporation from soil. USGS Water Supply Paper 659-A.
- Yao Y, Zheng C, Liu J, Cao G, Xiao H, Li H, Li W (2015) Conceptual and numerical models for groundwater flow in an arid inland river basin. *Hydrol Process* 29:1480–1492. <https://doi.org/10.1002/hyp.10276>
- Zhou Y, Li W (2011) A review of regional groundwater flow modeling. *Geosci Front* 2(2):205–214. <https://doi.org/10.1016/j.gsf.2011.03.003>